



A triboelectric nanogenerator as self-powered temperature sensor based on PVDF and PTFE

Kequan Xia¹ · Zhiyuan Zhu¹ · Hongze Zhang² · Zhiwei Xu¹

Received: 10 February 2018 / Accepted: 28 June 2018 / Published online: 4 July 2018
© Springer-Verlag GmbH Germany, part of Springer Nature 2018

Abstract

In this paper, we demonstrate a novel, light-weight, and flexible triboelectric nanogenerator (TENG) to serve as a self-powered temperature sensor. The triboelectric pairs consist of polytetrafluoroethylene and polyvinylidene fluoride and conductive copper foil is used as the conductive electrode. The output voltage of the temperature sensor increases linearly with increasing temperature. The temperature detection range is 10–90 °C and the response time and reset time of the sensor are approximately 0.01 and 3.5 s, respectively. Relatively simple and rapid fabrication of the temperature sensor offers the advantages of low cost and high practicality. The TENG has potential applications as a temperature sensor in the fields of environmental sciences, safety monitoring, and medical diagnostics.

1 Introduction

With the rapid development of portable electronic devices [1–3], temperature sensors capable of providing precise easy thermal monitoring have been widely studied and applied [4, 5]. Traditional temperature sensors rely on the continuous supply of chemical power, which limits the large-scale application of these sensors. Further, the reliance on an external power source prevents sensor networks from being built, particularly in extreme environments. In addition, the growing threat of global warming and the global energy crisis has stimulated the move towards self-powered sensors [6–8].

Recently, nanogenerators have been certified as self-powered devices that work and function without an external power supply. Moreover, nanogenerators have been widely used as sensors, such as self-powered temperature sensors based on thermoelectric generators [9–13] and piezoelectric nanogenerators [14]. However, conventional thermoelectric generator-based self-powered temperature sensors mainly rely on the Seebeck effect. Therefore, thermoelectric

generators do not work when the temperature of the heat source is spatially uniform or under time-dependent temperature fluctuations.

Fortunately, triboelectric nanogenerator (TENG), which has been proved to be able to harvest renewable energy in environment, draws much attention from all over the world [15–23]. In addition, TENG also has been widely utilized to make self-power sensor [15, 24–30]. Temperature sensor based on nanogenerator has been proposed [15]. However, its temperature detection range should be further expanded. In addition, the complicated fabrication process of TENG hinder its wide-ranging application [14, 31–36].

In this work, a novel, light-weight, and flexible self-powered temperature sensor based on the TENG is proposed. The triboelectric pairs consist of polytetrafluoroethylene (PTFE) and polyvinylidene fluoride (PVDF). Conductive copper foil serves as conductive electrode. Silicone paper and PVDF board are used as the supporting structure and the mechanism of the temperature sensor is based on dielectric constant changes [37]. The proposed temperature sensor can reflect temperature changes in real time in the temperature range of 10–90 °C. The response time and reset time of the sensor are approximately 0.01 and 3.5 s, respectively. The fabricated temperature sensor has the advantages of low cost and high practicality with potential applications in the fields of environmental sciences, safety monitoring, and medical diagnostics.

✉ Zhiyuan Zhu
zyzhu@zju.edu.cn

¹ Key Laboratory of Ocean Observation-Imaging Testbed of Zhejiang Province, Ocean College, Zhejiang University, No. 1 Zheda Road, Dinghai District, Zhoushan 316021, Zhejiang, People's Republic of China

² Nanjing Electronic Devices Institute, 524 East Zhongshan Road, Nanjing 210016, Jiangsu, People's Republic of China

2 Experimental

2.1 Material preparation

All materials used in this study are commercially available. The PVDF, PTFE, and copper foil were obtained from Packing Material Mall Corporation (Guangzhou, China). The PVDF and PTFE films were cleaned with deionized water followed by nitrogen (N_2) drying. The triboelectric pairs consist of PVDF and PTFE. Conductive copper foil is used as the conductive electrode. In addition, PVDF and silicone paper on the surface of the conductive copper foil tape act as a supporting structure.

2.2 Fabrication of triboelectric nanogenerator

The fabrication process of the TENG used as a self-powered temperature sensor is shown in Fig. 1. A piece of conductive copper tape was cut, and PTFE tape was attached to the surface of the conductive copper tape, as illustrated in Fig. 1a. A piece of PVDF board (6 cm \times 3 cm \times 1 mm) was also cut and another piece of conductive copper tape was attached

onto the bottom of the PVDF board, as shown in Fig. 1b. Finally, the whole device was folded into a half-arched shape and assembled, as shown in Fig. 1c.

2.3 Characterization

The electrical properties of the fabricated TENG were activated by tapping at a frequency of approximately 4 Hz. A digital oscilloscope (DSOX6004A, Keysight) was used to measure electronic performance. The morphology and microstructure of samples were examined under a scanning electron microscope (SEM; TM3000, Hitachi).

3 Results and discussion

Figure 2a shows a photograph of the fabricated TENG used as self-powered temperature sensor and representative SEM images of the PTFE and PVDF surfaces are presented in Fig. 2b, c. A hotplate was used as the heat source and the initial temperature and relative humidity of the experimental environment were 20 °C and 50%, respectively. The TENG device was used to detect changes in temperature via contact

Fig. 1 Fabrication of the TENG for use as a self-powered temperature sensor

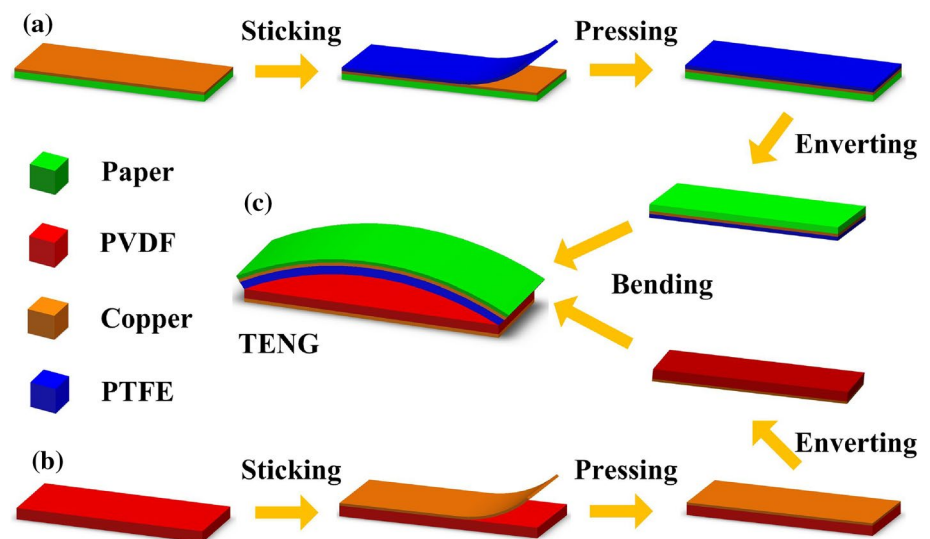
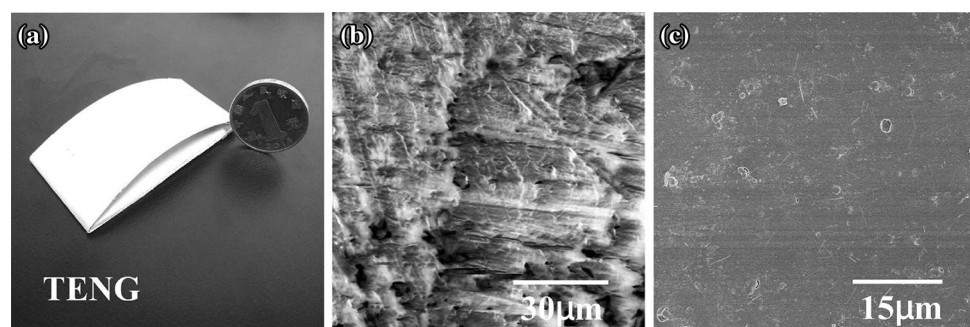


Fig. 2 a Photograph of the TENG fabricated for use as self-powered temperature sensor and SEM image of the surface of b PTFE and c PVDF

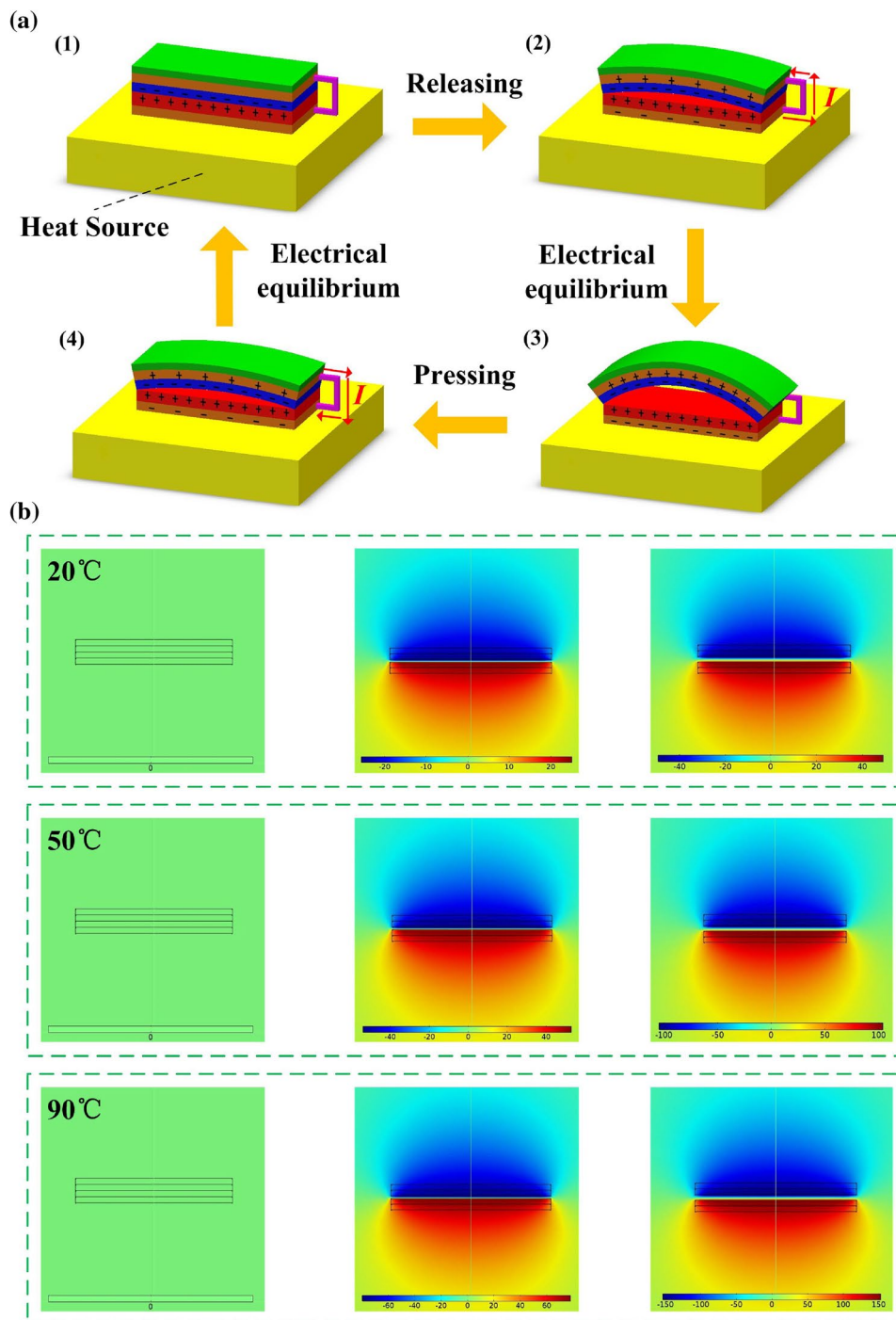


between the PVDF and heat source and the output voltages under different temperatures were then recorded.

The working mechanism of the TENG during one cycle is shown in Fig. 3. The PTFE is more attractive to electrons than PVDF, therefore electrons move from the PVDF to PTFE. Moreover, equal positive charges are produced on the surface of the PVDF, as is shown in Fig. 3a1. As the two types of material begin to separate, a potential difference is generated between the surfaces, which can induce

the transfer of charges between the conductive electrodes, as shown in Fig. 3a2. When PTFE approaches PVDF, a reverse potential difference is induced, which drives the flow of inductive electrons in the opposite direction, as shown in Fig. 3a3, a4. Therefore, the output voltage changes at different temperatures. To better understand this working mechanism, COMSOL Multiphysics software was used to simulate the potential distribution under open-circuit conditions for different temperatures, as illustrated in Fig. 3b.

Fig. 3 a Working mechanism of the TENG during one cycle. b Numerical calculations of the potential distribution across electrodes of the TENG at each step (1–3) under open-circuit conditions for different temperatures, as evaluated by COMSOL



To better understand the working mechanism, an equivalent theoretical model of the TENG was established based on the $V-Q-x$ relationship, as shown in Fig. 4. In the theoretical model, PTFE and paper can be regarded as two dielectric layers of different permittivity. The thickness of the PTFE and PVDF layers are set as d_1 and d_2 . The permittivity of PTFE, paper, and air are set as ϵ_1 , ϵ_2 and ϵ_0 . The contact area between the PTFE and paper is S and the distance between the two friction surfaces is set as $x(t)$. Then, the transferred charges induced by the potential difference are set as Q . So, the $V-Q-x$ theoretical equation for the TENG can be written as:

$$V = -\frac{Q}{S\epsilon_0} \left(\frac{d_1}{\epsilon_1} + \frac{d_2}{\epsilon_2} + x(t) \right) + \frac{\sigma x(t)}{\epsilon_0}.$$

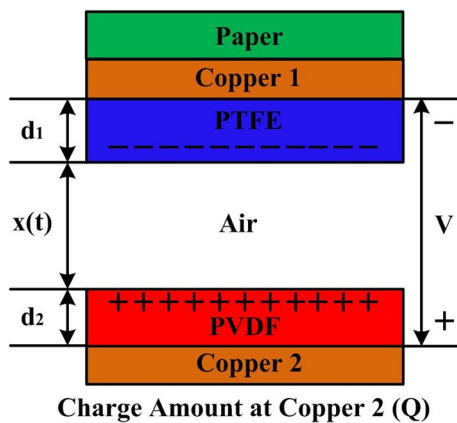


Fig. 4 Theoretical model of the TENG self-powered temperature sensor

When the temperature of the heat source increases, the permittivity of PTFE (ϵ_1) remains unchanged, whereas the permittivity of PVDF (ϵ_2) increases. Therefore, the output voltage (V) of the TENG increases.

More specifically, the device can be used to detect changes in temperature based on the contact between the PVDF and heat source. As the temperature of the heat source increases, the dielectric constant of PVDF also increases [38], whereas the dielectric constant of PTFE remains stable for temperatures between 10 and 100 °C [39]. The result is different output voltages of the TENG under different temperatures thereby emulating a temperature sensor.

Figure 5a shows the output voltage and output current when the loading resistance is increased from 100 kΩ to 150 MΩ. As the loading resistance increases, the output voltage of the device also increases, whereas the current drops due to the increase in resistance. The output power can be plotted as a function of the loading resistance, as shown in Fig. 5b. The maximum value of the output power reaches 240 μW at a loading resistance of 10 MΩ and the corresponding output voltage reaches 49 V, as shown in Fig. 5c. The stability of the TENG performance was also measured. The results show that the output performance of the device remains very stable after 10,000 cycles, as shown in Fig. 5d.

The fabricated TENG was attached to a heat source and the temperature of the heat source was controlled. The output voltage of the fabricated TENG for a load of 10 MΩ while attached to the heat source is shown in Fig. 6a. It can be seen that the output voltage increases as the temperature of the heat source increases. The temperature detection range is 10–90 °C. The output voltage of the TENG with a matched load of 10

Fig. 5 **a** Relationship between the output voltage/current and resistance of the external load. **b** Relationship between power and resistance to the external load for a maximum power of 240 μW and external load of 10 MΩ. **c** Corresponding output voltage. **d** Reliability of the fabricated TENG verified by the stable output voltage for 10,000 continuously working cycles

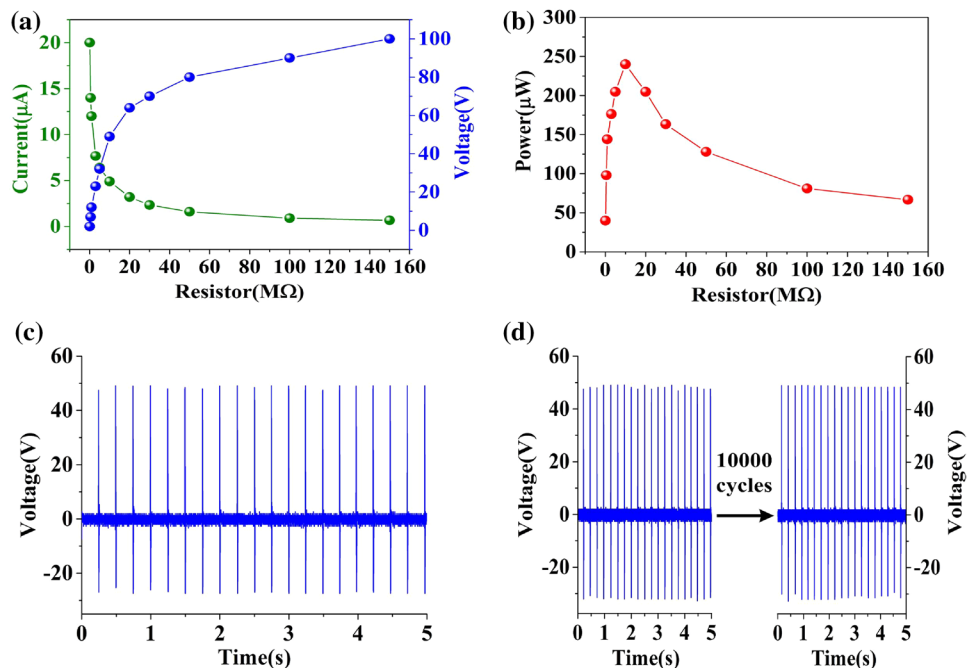
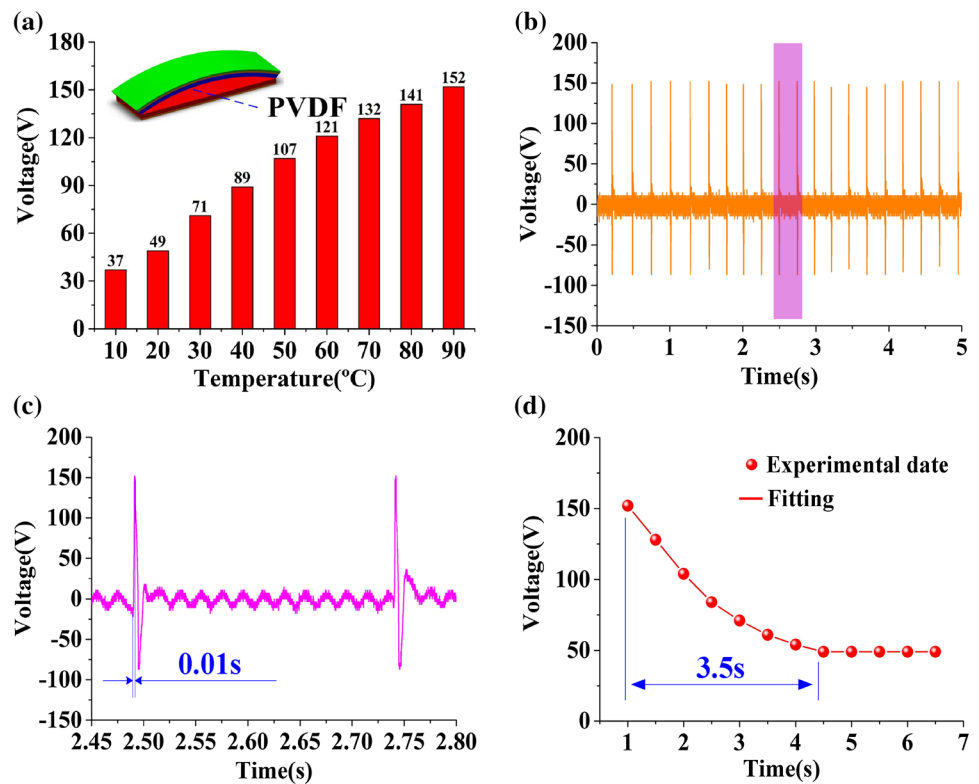


Fig. 6 **a** Dependence of the output voltage on the temperature of the heat source with a matched load of 10 M Ω . **b** Output voltage of the TENG with a matched load of 10 M Ω when the temperature of the heat source is 90 °C. **c** Enlarged output voltage pulse. **d** Output voltage of the TENG with a matched load of 10 M Ω at a temperature of 90 °C when the heat source is removed



M Ω when the temperature is 90 °C is shown in Fig. 6b. An enlarged positive output voltage pulse signal is observed, as shown in Fig. 6c. It can clearly be seen that the response time is approximately 0.01 s. In order to investigate the reset time of the temperature sensor, changes in the output voltage of the temperature sensor with a matched load of 10 M Ω at the temperature of 90 °C were studied with the heat source removed, as shown in Fig. 6d. The results show that the reset time of the temperature sensor is approximately 3.5 s.

Humidity was also shown to be an important factor in output performance of the device. At a temperature of 20 °C, the output voltage of the TENG with a load of 10 M Ω can reach 42, 37, and 32 V for a relative humidity of 70, 80, and 90%, respectively, as shown in Fig. 7a–c. It can be seen that the increase in relative humidity reduces the output performance of the device. Furthermore, the output voltage of the TENG with a load of 10 M Ω still changes with temperature at a humidity of 70, 80, and 90%, as shown in Fig. 7d–f. It is worth noting that the increase of relative humidity influences the output performance of the TENG. However, when used as self-powered temperature sensor, the proposed TENG can still indicate changes in temperature.

4 Conclusions

In this work, we proposed a novel, light-weight, and flexible self-powered temperature sensor based on proposed TENG that uses cost-effective materials such as PTFE, PVDF board, and conductive copper foil tape. Through testing, the output voltage of the temperature sensor was shown to increase linearly with temperature and the temperature detection range is 10–90 °C. The response time and reset time of the sensor are approximately 0.01 and 3.5 s, respectively. Furthermore, the influence of relative humidity on the output performance of the TENG used as self-powered temperature sensor was examined. Although humidity was shown influence the output performance, temperature changes can still be detected. The fabricated temperature sensor can be fabricated quickly and easily and has the advantages of low cost and high practicality. The proposed TENG can be used for potential applications in the fields of environmental sciences, safety monitoring, and medical diagnostics.

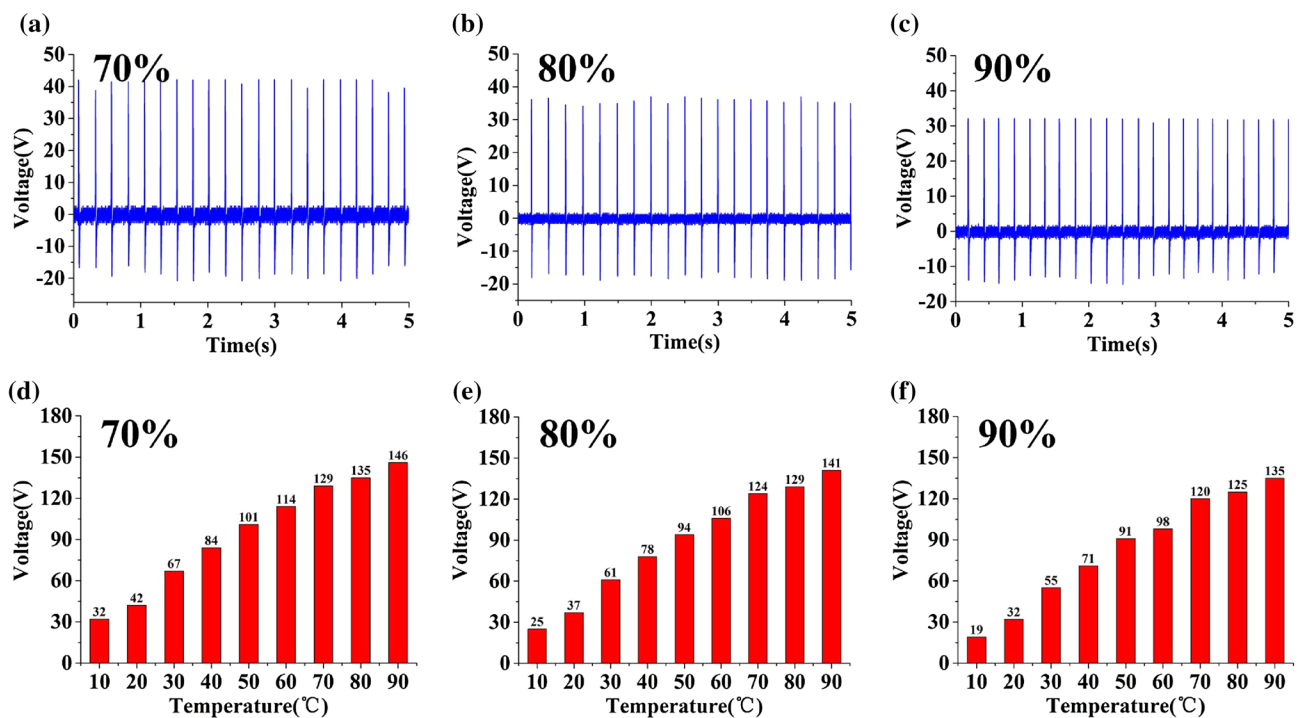


Fig. 7 a–c Output voltage and d–f dependence of output voltage on temperature of the heat source for the TENG acting as a self-powered temperature sensor with a matched load of 10 M Ω for a temperature of 20 °C and relative humidity of 70, 80, and 90%

Acknowledgements This work was supported by the Fundamental Research Funds for the Central Universities and National Natural Science Foundation of China (Grant nos. 61674218, 61731019). The authors would like to thank the Animal Science Experimental Teaching Center of Zhejiang University for SEM characterization.

References

1. D. Prasad, V. Nath, An ultra-low power high-performance CMOS temperature sensor with an inaccuracy of -0.3 °C/ $+0.1$ °C for aerospace applications. *Microsyst. Technol.* **24**(3), 1553–1563 (2018)
2. R. Kim, H.P. Chan, J.H. Moon, Development of a fiber-optic temperature sensor for remote measurement of the water temperature in a spent nuclear fuel pool. *J. Korean Phys. Soc.* **66**(10):1495–1498 (2015)
3. C. Lin, D. Zhang, X. Liu, A study of tin oxide thin film gas sensors with high oxygen vacancies. In *IEEE International Conference on Nano/Micro Engineered and Molecular Systems, 2012*. pp. 693–697
4. V. Kothari, B. Amna, K. Santosh, S. Lokendra, Fiber Bragg grating based temperature sensor for biomedical applications. In *Frontiers in Optics conference*, Washington, D.C., United States, September 2017 (2017), p. JTU2A.59
5. D. Niederberger et al., Portable electronic device with integrated temperature sensor. US20140321503A1, (2017)
6. H. Baer, M. Singer, *Global Warming and the Political Ecology of Health: Emerging Crises and Systemic Solutions*. (Routledge, London, 2016)
7. S. Clayton et al., Psychological research and global climate change. *Nat. Clim. Change* **5**(7), 640 (2015)
8. N. Watts et al., Health and climate change: policy responses to protect public health. *Lancet* **386**(10006), 1861–1914 (2015)
9. Z. Liu et al., Flexible piezoelectric nanogenerator in wearable self-powered active sensor for respiration and healthcare monitoring. *Semicond. Sci. Technol.* **32**(6), 064004 (2017)
10. H. Zhang et al., Simultaneously harvesting thermal and mechanical energies based on flexible hybrid nanogenerator for self-powered cathodic protection. *ACS Appl. Mater. Interfaces* **7**(51), 28142–28147 (2015)
11. H. Feng et al., Nanogenerator for biomedical applications. *Adv. Healthc. Mater.* **7**(10), 1701298 (2018)
12. H. Ouyang et al., Self-powered pulse sensor for antidiastole of cardiovascular disease. *Adv. Mater.* **29**(40), 1703456 (2017)
13. Q. Zheng et al., Recent progress on piezoelectric and triboelectric energy harvesters in biomedical systems. *Adv. Sci.* **4**(7), 1700029 (2017)
14. F. Xue et al., Piezotronic effect on ZnO nanowire film based temperature sensor. *ACS Appl. Mater. Interfaces* **6**(8), 5955–5961 (2014)
15. Y. Su et al., Low temperature dependence of triboelectric effect for energy harvesting and self-powered active sensing. *Appl. Phys. Lett.* **106**(1), 013114 (2015)
16. L. Zhao et al., A size-unlimited surface microstructure modification method for achieving high performance triboelectric nanogenerator. *Nano Energy* **28**, 172–178 (2016)
17. L. Xu et al., Coupled triboelectric nanogenerator networks for efficient water wave energy harvesting. *ACS Nano* **12**(2), 1849–1858 (2018)
18. B. Chen, Y. Yang, Z.L. Wang, Scavenging wind energy by triboelectric nanogenerators. *Adv. Energy Mater.* **8**(10), 1702649 (2017)

19. R. Liu et al., Shape memory polymers for body motion energy harvesting and self-powered mechanosensing. *Adv. Mater.* **30**(8), 1705195 (2018)
20. T. Guo et al., Compressible hexagonal-structured triboelectric nanogenerators for harvesting tire rotation energy. *Extreme Mech. Lett.* **18**, 1–8 (2018)
21. M. Xu et al., A soft and robust spring based triboelectric nanogenerator for harvesting arbitrary directional vibration energy and self-powered vibration sensing. *Adv. Energy Mater.* **8**(9), 1702432 (2017)
22. M. Han et al., r-Shaped hybrid nanogenerator with enhanced piezoelectricity. *ACS Nano* **7**(10), 8554–8560 (2013)
23. W.-S. Jung et al., High output piezo/triboelectric hybrid generator. *Sci. Rep.* **5**, 9309 (2015)
24. J. Chun et al., Highly anisotropic power generation in piezoelectric hemispheres composed stretchable composite film for self-powered motion sensor. *Nano Energy* **11**, 1–10 (2015)
25. Q. Jing et al., Self-powered triboelectric velocity sensor for dual-mode sensing of rectified linear and rotary motions. *Nano Energy* **10**, 305–312 (2014)
26. L. Lin et al., Transparent flexible nanogenerator as self-powered sensor for transportation monitoring. *Nano Energy* **2**(1), 75–81 (2013)
27. M. Xu et al., An aeroelastic flutter based triboelectric nanogenerator as a self-powered active wind speed sensor in harsh environment. *Extreme Mech. Lett.* **15**, 122–129 (2017)
28. Z.L. Wang, W. Wu, Piezotronics for sensors and energy technology. SPIE Newsroom (2014)
29. Z. Lin et al., Triboelectric nanogenerator enabled body sensor network for self-powered human heart-rate monitoring. *ACS Nano* **11**(9), 8830–8837 (2017)
30. J. Chen et al., Self-powered triboelectric micro liquid/gas flow sensor for microfluidics. *ACS Nano* **10**(8), 8104–8112 (2016)
31. Y. Yang et al., Single micro/nanowire pyroelectric nanogenerators as self-powered temperature sensors. *ACS Nano* **6**(9), 8456–8461 (2012)
32. Y. Yang et al., Nanowire-composite based flexible thermoelectric nanogenerators and self-powered temperature sensors. *Nano Res.* **5**(12), 888–895 (2012)
33. X. Wen et al., Applicability of triboelectric generator over a wide range of temperature. *Nano Energy* **4**, 150–156 (2014)
34. Y.-T. Jao et al., A self-powered temperature sensor based on silver telluride nanowires. *ECS J. Solid State Sci. Technol.* **6**(3), N3055–N3057 (2017)
35. Y. Xie et al., Flexible thermoelectric nanogenerator based on the MoS₂/graphene nanocomposite and its application for a self-powered temperature sensor. *Semicond. Sci. Technol.* **32**(4), 044003 (2017)
36. H. Zhang et al., Flexible pyroelectric generators for scavenging ambient thermal energy and as self-powered thermosensors. *Energy* **101**, 202–210 (2016)
37. S. Niu et al., Theoretical study of contact-mode triboelectric nanogenerators as an effective power source. *Energy Environ. Sci.* **6**(12), 3576–3583 (2013)
38. V.S. Yadav et al., The effect of frequency and temperature on dielectric properties of pure poly vinylidene fluoride (PVDF) thin films. In *Proceedings of the International Multiconference of Engineers and Computer Scientists* (2010), pp. 17–20
39. C.X. Lu et al., Temperature effect on performance of triboelectric nanogenerator. *Adv. Eng. Mater.* **19**(12), 1700275 (2017)